Design and Characterization of a Thyroid Hormone Receptor α (TRα)–Specific Agonist

2 AUTHORS:

Cory Antonio Ocasio

University of Sussex

12 PUBLICATIONS   **367** CITATIONS

SEE PROFILE

Thomas S Scanlan

Oregon Health and Science University

93 PUBLICATIONS   **5,508** CITATIONS

SEE PROFILE

Design and Characterization of a Thyroid Hormone Receptor α (TRα)-Specific Agonist

Cory A. Ocasio and Thomas S. Scanlan*

Chemistry and Chemical Biology Graduate Program and the Departments of Pharmaceutical Chemistry and Cellular & Molecular Pharmacology, University of California–San Francisco, 600 16th Street, San Francisco, California 94143-2280

Because of the extensive role of 3,5,3′-triiodo-L-thyronine (T_3) (Table 1) in vertebrate physiology, thyroid hormone analogues with tissue-specific actions, or selective thyromimetics, are highly desirable (1–3). T_3 exerts its actions by translocating into the nucleus of target cells and binding to the ligand binding domain of its cognate receptor, TR. Upon binding, TRs undergo a conformational change leading to recruitment of coregulator proteins and hence induction or repression of target gene transcription (4). TR is a member of the nuclear receptor superfamily, a group of ligand-activated transcription factors that are involved in a variety of cellular processes (4). There are two genes for TR, TRα and TRβ, that are differentially processed by alternative splicing or differential promoter usage, producing an ensemble of four different major isoforms (4, 5). Although most of these isoforms are ubiquitously expressed, the TR isoform ratio in some tissues is different, giving rise to tissue-specific isoform actions (5, 6).

Selective thyromimetics bind to and preferentially activate or inactivate one of three physiologically relevant TR subtypes: $TR\alpha_1$, $TR\beta_1$, and $TR\beta_2$. A complete panel of thyromimetics that either activate or inactivate these receptor subtypes would provide a set of chemical tools that may assist in understanding the molecular-level basis behind TR physiology.

RESULTS AND DISCUSSION

The genesis of CO23 (Table 1) came about by first looking at a class of structurally related compounds, the TRβ-selective agonists (3, 7–11). All of these compounds were derivatized from the thyronine backbone of T_3 by modifying either the moiety in the C_1 region of the scaffold, consisting of a linker capped by an acid group (i.e., carboxylic, oxamic, and malonamic acids), or both the C_1 region and the 3′ position of the outer ring; it has been shown that placing large hydrophobic groups

ABSTRACT Thyroid hormone is a classical endocrine signaling molecule that regulates a diverse array of physiological processes ranging from energy metabolism to cardiac performance. The active form of thyroid hormone, 3,5,3′-triiodo-L-thyronine or T_3, exerts many of its actions through its receptor, the thyroid hormone receptor (TR), of which there are two subtypes for two isoforms: $TR\alpha_1$, $TR\alpha_2$, $TR\beta_1$, and $TR\beta_2$. Although TR isoforms, with the exception of $TR\beta_2$, are expressed in all tissues, they display different patterns of expression in different tissues, giving rise to tissue-specific isoform actions. Currently, several TRβ-selective agonists have been developed; however, TRα-selective agonists have remained elusive. Herein, we report the synthesis and biological evaluation of CO23, the first potent thyromimetic with TRα-specific effects *in vitro* and *in vivo*.
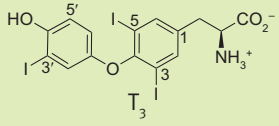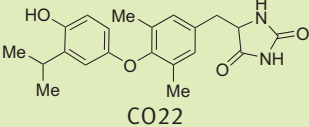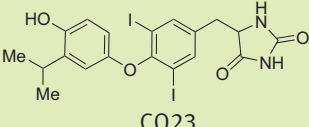
*Corresponding author,
scanlan@cgl.ucsf.edu.

TABLE 1. Binding affinity and potency of CO22 and CO23

Compound	K_d and EC$_{50}$ values (nM)					
	Binding affinity $(K_d)^a$		Transactivation in U2OS cells $(EC_{50})^b$		Transactivation in HeLa cells $(EC_{50})^b$	
	TRα	TRβ	TRα	TRβ	TRα	TRβ
T$_3$	0.058	0.081	2.4 ± 0.4	11 ± 2	2.4 ± 0.5	2.4 ± 0.5
CO22	286 ± 27	280 ± 102	3870 ± 1	c	c	c
CO23	1.2 ± 0.2	1.7 ± 0.3	34 ± 4	390 ± 3	11 ± 1	58 ± 1

^{a}Determined by means of an ^{125}I-T$_3$ competitive binding assay, and data are reported as the mean K_d ± standard error of the mean, $n = 3$. ^{b}Determined through use of a TRE-driven dual-luciferase reporter assay in U2OS or HeLa cells, and the data are reported as the mean EC$_{50}$ value ± standard error of the mean, $n = 3$ (T$_3$, CO22, and CO23 in HeLa cells) and $n = 6$ (CO23 in U2OS cells). ^{c}Not applicable.

in the 3′ position improves the β-selectivity for this class of thyromimetic (8). It has also been reported that compounds with a phenyl-naphthylene core bind to TRβ in the sub-nanomolar range and display low to modest selectivity for TRβ. Interestingly, these thyromimetics are the first to display a structure activity relationship that diverges from other thyromimetics that are based on the biaryl ether core found in the thyronine backbone of T$_3$ (12).

After surveying a list of β-selective agonists, we observed that heterocycles were underutilized in generating chemical diversity at the C$_1$ region, with few exceptions (10, 11, 13). Recent examples of thyromimetics with heterocycles in the C$_1$ region and outer ring include thyromimetics that incorporate inner-ring fused quinoline-2-carboxylates and indole-2-carboxylates in the C$_1$ region and indoles and indazoles forming heterocyle-fused outer rings (14, 15). Despite these examples, thyromimetics containing heterocycles are rare, and hence the infrequent use of heterocycles in thyromimetic design coupled with their relatively low cost and availability, chemical diversity (particularly with

respect to pK_a), and ease of synthetic incorporation into the C$_1$ region prompted the synthesis of a small panel of thyroid hormone analogues bearing heterocycles at the 1 position with or without a linker. The halogen-free 3,5-dimethyl,3′-isopropyl inner- and outer-ring substitution pattern was selected for this collection of thyroid hormone analogues due to ease of synthesis.

An *in vitro* evaluation of a small panel of thyroid hormone analogues identified one lead compound, CO22 (Table 1), that displays modest binding affinity and potency but at the highest concentration is as efficacious as T$_3$ when tested for TRα-induced transactivation in U2OS cells (Table 1 and Figure 1, panels a and b). CO22 showed significantly lower potency and efficacy when assayed for TRβ-induced transactivation. In fact, at the highest concentration tested, transcriptional activity did not plateau, and it displayed about half the efficacy of T$_3$, indicating that CO22 is a poor agonist against TRβ (Table 1 and Figure 1, panels a and b).

The structure–activity data revealed a way to circumvent the problem in potency of CO22. A similar thyroid

a

b

c

d

e
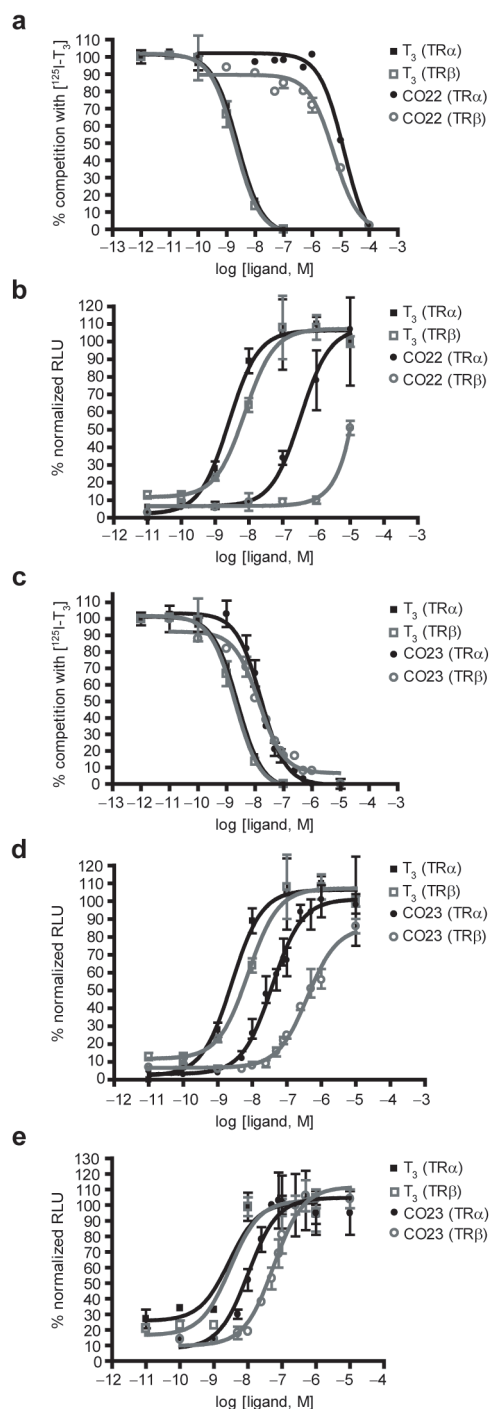
hormone analogue displaying an EC_{50} value of ~6 nM when tested for TRα-induced transactivation in COS-1 cells is different from CO22 in two ways: 1) there is a thiazolidinedione in the C_1 region instead of an imidazolidinedione and 2) the inner ring consists of iodides rather than methyl groups (11). Although this compound is structurally similar to CO23, it is unknown whether this compound displays TRα specificity *in vitro* because it was not tested for TRβ-induced transactivation in COS-1 cells. In terms of CO23, the imidazolidinedione was deemed necessary for conferring TRα-specificity, and thus we modified the inner ring of CO22 by replacing the methyl groups with iodides (Scheme 1).

CO23 proved superior to CO22 with respect to binding and transactivation because it exhibits a >200-fold improvement in binding affinity as well as a >100-fold improvement in potency (as determined by transactivation in U2OS cells) compared with CO22 (Table 1 and Figure 1, panels a–d). Although CO23, like CO22, shows no preference in binding to $TRα_1$ in an ^{125}I-T_3 competitive binding assay, it shows selective activation of $TRα_1$ in a DR4-driven dual-luciferase reporter assay using U2OS cells (Table 1 and Figure 1, panels c and d). Note that the replacement of the inner-ring methyl groups with iodides results in diminished TRα selectivity (Figure 1, panel d). It is likely that the polarizability and increased electronegativity of iodides favor binding to the TR binding pocket in a steric and electronic sense, making it more potent to both receptors. However, the methyl groups, which are smaller and less polarizable and electronegative than iodides, may cause negative interactions that decrease both binding affinity and transactivation through TR but affect TRα activation to a lesser extent than TRβ activation. With this in mind, modification of the inner-ring substituents may serve to optimize the selectivity of an already selective thyromi-

Figure 1. *In vitro* evaluation of CO22 and CO23. a, c) ^{125}I-T_3 competitive binding curves for T_3, CO22, and CO23 against $hTRα_1$ and $hTRβ_1$; b, d) a TRE-driven dual-luciferase reporter assay showing transactivation curves for T_3, CO22, and CO23 against $hTRα_1$ and $hTRβ_1$ in U2OS cells; e) A TRE-driven dual-luciferase reporter assay showing transactivation curves for T_3 and CO23 against $hTRα_1$ and $hTRβ_1$ in HeLa cells. Plots show mean of triplicates with standard deviation.
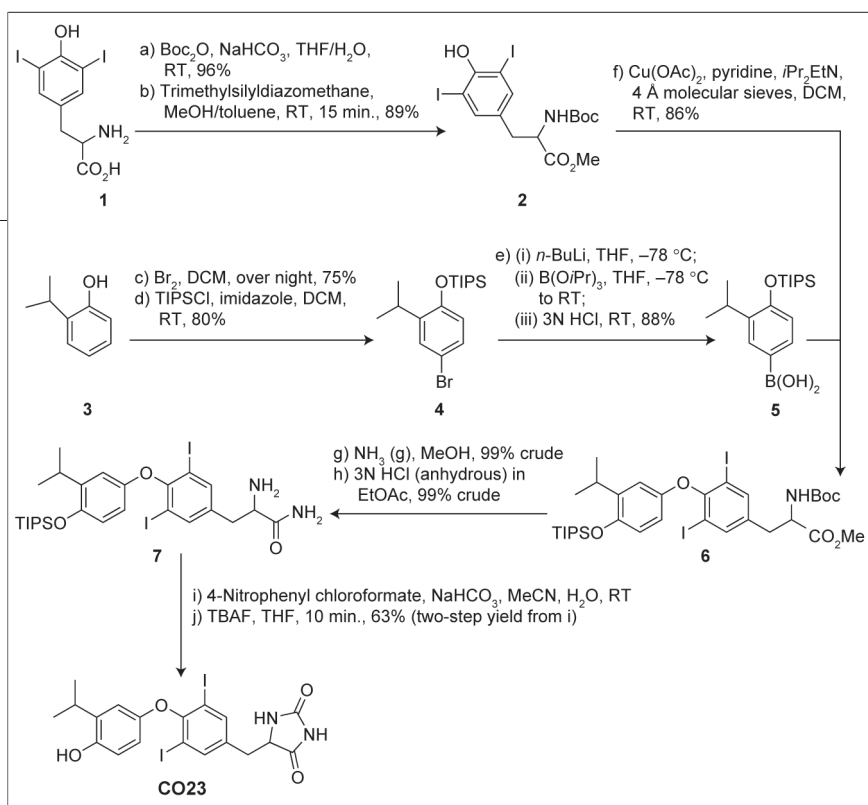
Scheme 1. Synthesis of CO23.

metic, whereas the C_1 moiety may be responsible for setting the selectivity of a thyromimetic for TRα or TRβ.

When determining selective activation of TRs using this cell line, it is necessary to compare the potency of the test ligand to the control ligand T_3 because T_3 shows a difference in activation of TRα_1 and TRβ_1 using a synthetic TRE-driven luciferase reporter construct; CO23 selectively activated TRα_1 by ~3-fold in U2OS cells relative to T_3 (Table 1 and Figure 1, panel d). Due to this difference in T_3 activation of TRα_1 and TRβ_1 in U2OS cells, it was necessary to directly determine the TRα_1 selectivity of CO23. In HeLa cells, a cell line where T_3 is equipotent with respect to TRα_1 and TRβ_1 activation, CO23 showed a ~5-fold preference in TRα_1 activation (Table 1 and Figure 1, panel e).
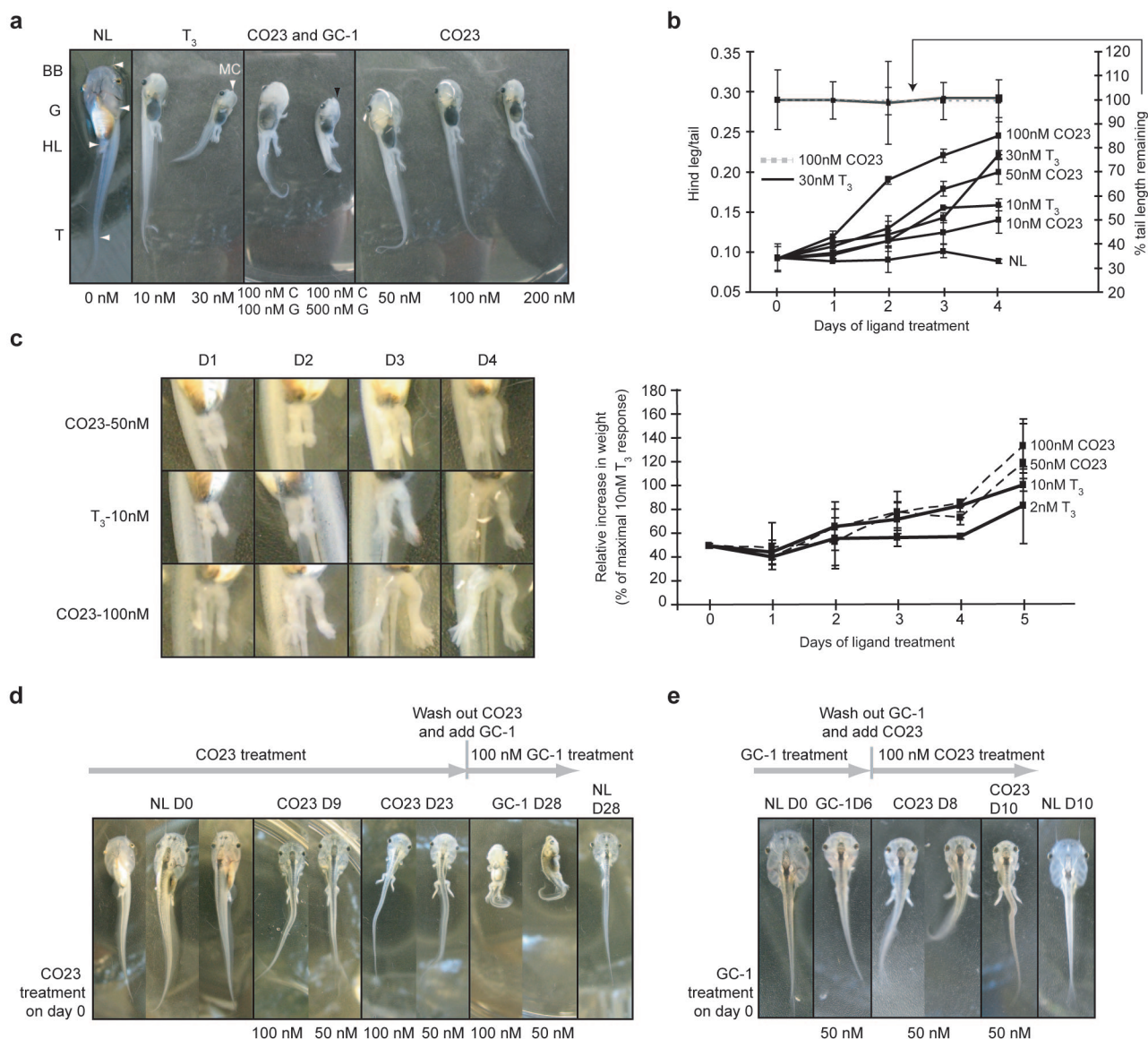
After the TRα selectivity of CO23 was established *in vitro*, CO23 was further investigated in precociously induced amphibian metamorphosis. Amphibian metamorphosis occurs in three distinct stages: premetamorphosis, prometamorphosis, and climax (*16*). The premetamorphic tadpole primarily undergoes larval growth; however, the onset of prometamorphosis is marked by secretion of thyroid hormone from the developing thyroid gland, giving rise to a number of morphological and biochemical changes such as hind limb (HL) proliferation, differentiation, and induction of genes, including TRβ (*16, 17*). Fore leg emergence and the rapid and complete resorption of gills and tail mark metamorphic climax and, thus, complete the developmental program (*16, 17*).

Using *Xenopus laevis* metamorphosis as a model system for studying biologically active and selective thyroid hormone agonists offers several advantages. First, *Xenopus* and mammalian TRs, their heterodimer partners, and the receptor-associated coregulators are structurally and functionally well conserved (*17*). Furthermore, *Xenopus* metamorphosis has been extensively studied, and detailed molecular events throughout the process are well known (*17*). *Xenopus* TRα (xTRα) is expressed early on in the developing embryo and before the larval tadpole has a functional thyroid gland (*17, 18*). Just prior to metamorphosis, xTRα expression becomes widespread with locally high levels occurring in tissues that are destined to undergo proliferation and differentiation such as the limb buds, brain, and skin (*17, 18*). The gene for TRβ is itself an early-response gene of thyroid hormone, and its messenger RNA levels increase as thyroid hormone levels increase during the progression of metamorphosis, reaching a peak at metamorphic climax where death and resorption of larval tissue predominate (*16, 19*). This correlation between metamorphic stage, TR-isoform expression, and morphogenic response is ideal for the study of a TRα-selective thyromimetic.

Stage-53/54 tadpoles treated with CO23 (50, 100, and 200 nM) experienced HL growth as extensive as or greater than that of tadpoles treated with 30 nM T_3 after 1 week (Figure 2, panel a). In addition, CO23-treated tadpoles exhibited less tail, gill, and head resorption at concentrations (50 and 100 nM) that yielded greater or equal HL growth as compared with 30 nM T_3-treated tadpoles (Figure 2, panel a). In a 4-d time course, tadpoles treated with CO23 (50, 100, and 200 nM) showed more extensive HL development after each successive day compared with tadpoles treated with 30 nM T_3 (Supplementary Figure 1, panels a and b). Treating tadpoles in a dose-dependent manner with T_3 (10, 20, and 30 nM) and CO23 (10, 50, 100, 200, and 300 nM) showed that after 4 d, concentrations of up to 200 nM CO23 were more effective than or as effective as 30 nM T_3 in promoting HL development. The same CO23-treated tadpoles displayed less head and tail resorption as did 30 nM T_3-treated tadpoles (Supplementary Figure 2, panel a). Furthermore, to show that CO23 works through

Figure 2. *In vivo* analysis of CO23. a) Induced metamorphosis of stage-53/54 tadpoles, *n* = 3, treated for 7 d with vehicle, T₃ (10 and 30 nM), CO23 (50, 100, and 200 nM), and a combination of CO23 (100 nM) and GC-1 (100 and 500 nM); b, c) HL development of tadpoles, *n* = 3, treated without b) and with c) 1 mM methimazole and vehicle, T₃ (2, 10, and 30 nM), and CO23 (10, 50, and 100 nM) up to 4 d as measured by H/T ratio (b) or relative increase in weight (c, represented as a percentage of the maximal T₃ response); d) tadpoles were treated with vehicle for 28 d and 50 and 100 nM CO23 for 23 d, then placed in 100 nM GC-1 for 5 d more. NL, vehicle control; e) tadpoles were treated with vehicle for 10 d and 50 nM GC-1 for 6 d, then placed in 100 nM CO23 for 4 d more. All images are to scale for ease of comparison.

TR, tadpoles were treated with CO23 and NH-3, a TR antagonist (*17*). Tadpoles treated with 100 nM CO23 and 500 nM NH-3 displayed less HL and fore leg development and resorption compared with the CO23-treated control and only slightly more HL development compared with the no ligand control after 5 d (Supplementary Figure 2, panel b).

A combination experiment whereby stage-53/54 tadpoles were subjected to 100 nM CO23 and the TRβ-selective agonist GC-1 (100 or 500 nM) showed that tad-
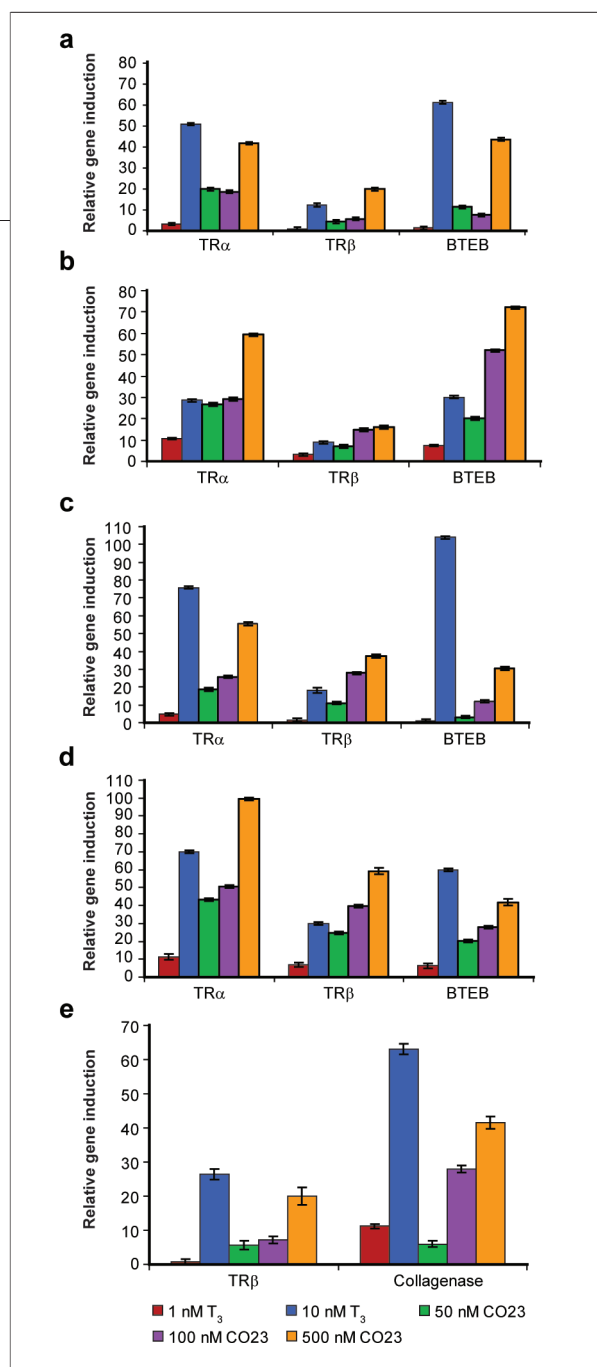
Figure 3. Relative gene induction as determined by quantitative PCR. a, b) Relative gene induction by T_3 and CO23 in HL tissue after 2 (a) and 6 (b) d of treatment; c, d) relative gene induction by T_3 and CO23 in head tissue after 2 (c) and 6 (d) d of treatment; e) relative gene induction by T_3 and CO23 in tail tissue after 6 d of treatment.

poles treated with CO23 and a low dose of GC-1 resembled 10 nM T_3-treated tadpoles and tadpoles treated with CO23 and a high dose of GC-1 resembled 30 nM T_3-treated tadpoles (7, 17) (Figure 2, panel a). Therefore, this combination treatment rescues the β-isoform effects (resorption of gills, head, and bar bells, reorganization of the brain, and development of Meckel's cartilage in the jaw area) at the CO23 concentration tested.

The effects of CO23 on HL development were further explored by measuring the length and mass of growing HLs in response to CO23 and T_3 treatment. In the first experiment, tadpoles treated with 100 nM CO23 yielded the longest limbs after each successive day up to 4 d, whereas the progression in length of 50 nM CO23-treated tadpole limbs was similar to that of 30 nM T_3-treated tadpole limbs. At low concentrations of T_3 and CO23 (10 nM), HL lengthening was less rapid and extensive compared with the no ligand control (Figure 2, panel b). In the presence of a thyroid hormone biosynthesis inhibitor (methimazole), the HLs of CO23 (50 and 100 nM)-treated tadpoles grew more rapidly than (100 nM CO23) or in similar fashion (50 nM CO23) to those of 10 nM T_3-treated tadpoles (Figure 2, panel c). It should be noted that 1 mM methimazole renders tadpoles much more sensitive to T_3.

Further studies with CO23 and GC-1 indicated that sequential treatment with isoform-selective agonists can temporally control tadpole morphogenesis. Treating tadpoles with CO23 (50 and 100 nM) for up to 23 d led to massive HL growth with slight resorption of head and gills, and replacing it with 100 nM GC-1 on the 23rd day led to the rapid resorption of head and tail, shrinking of body size, and a hunch-back appearance after 5 d of treatment (Figure 2, panel d). Conversely, treating with 50 nM GC-1 and replacing it with 100 nM CO23 yielded opposite results, although some limb growth did occur with GC-1 (Figure 2, panel e). In fact, limb growth resulting from GC-1 may be attributed to GC-1 activation of TRα. This is likely because in the early stages of tadpole metamorphosis TRα is the most abundant isoform present and its activation leads to induction of TRβ, which then carries out the β-isoform effects upon activation by GC-1.

Next, we sought evidence for the TRα specificity of CO23 by monitoring induction of early and late thyroid hormone responsive genes. This was done by performing quantitative real-time polymerase chain reaction (rt-PCR) on complementary DNAs derived from various *Xenopus* tissues. TRβ and xBTEB, a zinc-finger transcription factor, are early response genes that are both rapidly induced by T_3, and in the case of xBTEB, by GC-1 as well (17, 18). As such, xBTEB can be viewed as a TRβ-induced early gene, and hence, its induction by CO23 should be less intense compared with that by T_3. The next gene of interest, collagenase-3, is a late responsive gene that is up-regulated in tail tissue and should not

respond to CO23 as effectively as to T_3, particularly on day 6 (*19*). In this experiment, CO23 acted as hypothesized; in HL and head tissue after 2 and 6 d of treatment, CO23 (100 and 500 nM)-induced TRβ levels were higher than those induced by T_3 (10 nM), except in HL tissue treated with 100 nM CO23 for 2 d (Figure 3, panels a–d). In terms of xBTEB induction, CO23 (50, 100, and 500 nM) is less effective than T_3 (10 nM) (Figure 3, panels a, c, and d). It is only in HL tissue after 6 d of treatment (late prometamorphosis) that CO23 (100 and 500 nM) induced xBTEB more effectively than T_3 (Figure 3, panel b). Up-regulation of the late response gene collagenase-3 by CO23 is also less effective at all

concentrations compared with that by T_3 (10 nM) (Figure 3, panel e). As for xTRα, only the highest dose of CO23 (500 nM) was as effective as T_3 (10 nM) at its up-regulation.

CO23 is the first thyroid hormone analogue to demonstrate TRα specificity *in vitro* and *in vivo*. The implications of this may extend to mammalian species because $TRα_1$ in mammals is known to regulate several cardiac parameters that maintain healthy cardiac performance. Finally, CO23, along with current thyromimetics, may serve as chemical probes of TR signaling pathways, leading to new insights regarding TR biology.

EXPERIMENTAL METHODS

General Synthesis. All chemicals used for organic synthesis were purchased from Aldrich, Sigma-Aldrich, Fluka, or Acros and were used without further purification. Anhydrous conditions were maintained under argon using standard Schlenk line techniques and oven-dried glassware. Anhydrous tetrahydrofuran (THF), dichloromethane (DCM), pyridine, and diisopropyl ethylamine were available in house and dispensable from a solvent purification system. Compounds were purified by either flash chromatography using silica gel (VWR Scientific) or preparatory thin layer chromatography (prep TLC) using Analtech prep TLC plates (20 cm × 20 cm, 1000 μm). ^1H NMR spectra were taken on the Varian Utility 400 MHz spectrometer in $CDCl_3$ or DMSO-d_6 solvents, and chemical shifts were reported as δ (parts per million) downfield of the internal control, trimethylsilane (TMS), for all solvents. High-resolution mass spectrometry (HRMS) using electrospray ionization was performed by the National Bio-Organic, Biomedical Mass Spectrometry Resource at UCSF, and specific rotation was determined using a Perkin Elmer 241 polarimeter. Purity of final compounds was assessed using Rainin HPXL pumps, an Altech Nucleosil 100 (C_{18}) 10 μm 4.6 mm × 250 mm column with a 7.5 mm guard column, and a Varian ProStar 330 photo diode array detector controlled by a Varian Star chromatography workstation. HPLC grade acetonitrile and H_2O were purchased from Fisher.

Synthesis of CO23. Replacement of the inner-ring methyl groups with iodides was accomplished by coupling of a Boc-protected diiodotyrosine methyl ester, **9**, with a triisopropylsilyl (TIPS)-protected 4-hydroxy-3-isopropylphenyl boronic acid, **12**, resulting in the biaryl ether intermediate **13** (*20–23*). Subsequent amidation of the methyl ester and deprotection of the Boc group set up the amino acid amide side chain for cyclization into the imidazolidinedione by 4-nitrophenyl chloroformate and water (*20, 24, 25*). The synthesis of CO23 was finalized by deprotection of the TIPS group with tetrabutylammonium fluoride (*20*) (Scheme 1). Full experimental details for both CO22 and CO23 are described in Supplementary Methods. Analytical data for CO22 and CO23 are as follows. CO22 ^1H NMR (400MHz, $CDCl_3$): δ 1.21 (d, 6H, $J = 8.0$ Hz), 2.10 (s, 6H), 2.75 (dd, 1H, $J = 4.0$ Hz, $J = 12.0$ Hz), 3.14 (heptet, 1H, $J = 8.0$ Hz), 3.22 (dd, 1H, $J = 8.0$ Hz, $J = 12.0$ Hz), 4.28 (dd, 1H, $J = 4.0$ Hz, $J = 8.0$ Hz), 4.97 (s, 1H), 5.57 (s, 1H), 6.22 (dd, 1H, $J = 4.0$ Hz, $J = 8.0$ Hz), 6.58 (d, 1H, $J = 8.0$ Hz), 6.73 (d, 1H, $J = 4.0$ Hz), 6.91 (s, 2H), 7.27 (s, 1H). CO22 HRMS (*m/z*): [M]$^+$ calcd for $C_{21}H_{24}N_2O_4$, 368.1736; found, 368.1749. CO22 HPLC (MeCN/water,

65–100%, 12 min): retention time 3.6 min; 99% pure. CO23 [α]$^{20}_D$ = −18.7 (*c* 0.05, MeOH). CO23 ^1H NMR (400MHz, DMSO-d_6): δ 1.11 (d, 6H, $J = 8.0$ Hz), 2.81 (dd, 1H, $J = 8.0$ Hz, $J = 14.0$ Hz), 2.93 (dd, 1H, $J = 4.0$ Hz, $J = 14.0$ Hz), 3.15 (heptet, 1H, $J = 8.0$ Hz), 4.35 (dd, 1H, $J = 4.0$ Hz, $J = 8.0$ Hz), 6.16 (dd, 1H, $J = 4.0$ Hz, $J = 8.0$ Hz), 6.61 (d, 1H, $J = 8.0$ Hz), 6.63 (d, 1H, $J = 4.0$ Hz), 7.75 (s, 2H), 7.98 (s, 1H), 8.96 (s, 1H), 10.60 (s, 1H). CO23 HRMS (*m/z*): [M]$^+$ calcd for $C_{19}H_{18}I_2N_2O_4$, 591.9356; found, 591.9356. CO23 HPLC (MeCN/water, 65–100%, 12 min): retention time 3.9 min; 99% pure.

Thyroid Hormone Competition Binding Assay. Full-length $hTRα_1$ and $hTRβ_1$ were expressed using a TNT T7 quick-coupled transcription translation system (Promega). Competition assays for binding of unlabeled T3 and CO23 were performed using 1 nM ^{125}I-T_3 in a gel filtration binding assay as described (*26*).

Transient Transfection Assays. Human bone osteosarcoma epithelial (U2OS) cells or human uterine cervical cancer (HeLa) cells (Cell Culture Facility, UCSF) were grown to ~80% confluency in Dulbecco's modified Eagles (DME)/H-21, 4.5 g L^{-1} glucose medium containing 10% newborn calf serum (NCS) or fetal bovine serum (FBS), respectively (both heat-inactivated), 2 mM glutamine, 50 units mL^{-1} penicillin, and 50 μg mL^{-1} streptomycin. Cells ((~1.5–2) × 10^6) were collected and resuspended in 0.5 mL of electroporation buffer (Dulbecco's phosphate-buffered saline (PBS) containing 0.1% glucose and 10 mg mL^{-1} bioprene) with 1.5 μg of a TR expression vector (full-length $hTRα_1$–CMV or $hTRβ_1$–CMV), 0.5 μg of pRL-TK constitutive *Renilla* luciferase reporter plasmid (Promega), 5 μg of a reporter plasmid containing a synthetic TR response element (DR-4) containing two copies of a direct repeat spaced by four nucleotides (AGGTCAcaggAGGTCA) cloned immediately upstream of a minimal thymidine kinase promoter linked to a luciferase coding sequence (*7*). Cells were electroporated using a Bio-Rad gene pulser at 350 V and 960 μF in 0.4 cm cuvettes, pooled in DME/F-12 Ham's 1:1 without phenol red (U2OS) or DME/H-21 (HeLa), supplemented as above except that NCS and FBS were hormone-stripped using dextrose-coated charcoal, and plated in 96-well (U2OS) or 12-well (HeLa) plates to a final density of 20,000 cells per well and 100,000 cells per well, respectively. After a 2-h incubation period, compounds in 1% DMSO were added to the cell culture medium in triplicate. After an additional 16-h incubation period, cells were harvested and assayed for luciferase activity using the Promega dual-luciferase kit (Promega) and an Analyst AD (Molecular Devices). Data normalized to the *Renilla* internal control were analyzed

with GraphPad Prism, v4, using the sigmoid dose response model to generate EC_{50} values; EC_{50} values were obtained by fitting data to the following equation: $Y = \text{bottom} + (\text{top} - \text{bottom})/(1 + 10^{(\log EC50 - X)} \times \text{HillSlope}))$.

Preparation of Chemicals. Stocks of T_3, CO23, GC-1, and NH-3 were prepared with DMSO at a concentration of 10 mM and stored at -20 °C until use; GC-1 and NH-3 were prepared as described previously (27, 28). All other chemicals were purchased from Sigma unless otherwise indicated. Methimazole (Aldrich) was dissolved in sterile water to a final concentration of 1 M and stored at -20 °C. Aminobenzoic acid ethyl ester (0.1%, Tricaine or MS222) was made fresh in sterile ddH_2O and kept at 4 °C for no longer than 1 week.

General *X. laevis* Tadpole Procedures. *X. laevis* stage-53/54 tadpoles were purchased from NASCO, Inc., and staged according to Nieuwkoop and Faber (29). Upon receipt, tadpoles were allowed to set overnight at RT (18–25 °C) in order to recover from shipping shock, after which half of the initial rearing water was replaced with $0.1\times$ Marc's Modified Ringer's (MMR) buffer ($10\times$ solution consists of 100 mM NaCl (Fisher), 2 mM KCl (Fisher), 1 mM $MgCl_2$, 2 mM $CaCl_2$, 0.1 mM EDTA, and 5 mM *N*-2-hydroxyethylpiperazine-*N*′-2-ethanesulfonic acid, pH 7.8) and in some cases, the tadpoles were maintained at a concentration of 1 mM methimazole. Tadpoles were ultimately maintained in fresh $0.1\times$ MMR buffer, changed every 2 d, with or without methimazole. After completion of experiments, live tadpoles were euthanized by treatment with 0.01% Tricaine, exposure to an ice bath, and either fixation in PBS containing 3.5% formalin or decapitation in order to ensure death. Animals were photographed with a Canon PowerShot A510, and images were processed with Adobe Photoshop CS, v8, and Adobe Illustrator CS, v11. All tadpole experiments were conducted in accordance with Institutional Animal Care and Use Committee approval (animal protocol no. A7228-23070-01).

Induced Metamorphosis Experiments. Stage-53/54 tadpoles were added to extra-deep Petri dishes (Fisher) in triplicate containing 50 mL of $0.1\times$ MMR buffer and vehicle or the appropriate concentration(s) and combination of ligand(s) (T_3, CO23, GC-1, and NH-3) with or without methimazole. The final DMSO concentration was 0.1%. Induced metamorphosis experiments were repeated at least three times.

Quantification of HL Development. Groups of tadpoles were treated with the appropriate concentration of ligand and photographed live daily, every 24 h, for 4 d or sacrificed before excision of HLs. One method of quantifying HL development was through measuring the HL length (pixels) to tail length (pixels) (H/T) ratio, because this ratio correlates reasonably well with metamorphic stage and serves to normalize for differences in initial tadpole size (30). The percentage of tail length remaining was also determined for the highest ligand concentrations tested (30 nM T_3 and 100 nM CO23) in order to show that tail length remains constant and, thus, leaves the H/T ratio unaffected. These experiments were repeated twice, and each experimental point consisted of the mean H/T ratio and percent tail length remaining for three tadpoles. HL development was also monitored by recording the increase in mass as compared with day zero of HLs over a 4 d time period. Tadpole HLs from different groups of tadpoles in 1 mM methimazole were excised every 24 h, placed on pretared weighing paper, dried in ambient air for 3 h, and then weighed on a Sartorius balance accurate to 0.01 mg. These experiments were repeated twice, and each experimental point consisted of the mean increase in weight normalized to maximal T_3 response for three to five tadpoles.

Temporal Control Over Morphogenesis. These experiments were carried out in the presence of 1 mM methimazole as in induced metamorphosis experiments except that at the indicated time point, $0.1\times$ MMR buffer containing either CO23 (50 and 100 nM) or GC-1 (50 nM) was replaced with $0.1\times$ MMR containing GC-1 (50 nM) or CO23 (100 nM), respectively. Each experimental point consisted of three tadpoles, and each experiment was repeated twice.

Quantitative rt-PCR Assay. Total RNA was extracted from head, HL, and tail tissue from groups of 6–10 tadpoles using TRIzol reagent (Invitrogen) according to the manufacturer's specifications. The total RNA was processed as described previously (13), and the C_T method (Applied Biosystems User Bulletin no. 2) was employed to quantify gene induction normalized to the *Xenopus* 18S ribosomal RNA subunit (RL8) and relative to a physiological calibrator. Relative gene induction was quantified with the equation $2^{-\Delta\Delta CT}$ in sextuplicate, and the standard deviation was calculated using the comparative method described in User Bulletin no. 2. rt-PCR reactions were carried out on a DNA Engine Opticon2, and the data were analyzed using Opticon software. Primers used to detect RL8 and collagenase-3 were the same as reported previously (13). Primers used to detect all other target genes were designed using the Primer3 website (http://frodo.wi.mit.edu/cgi-bin/primer3/primer3_www.cgi), and the sequences are as follows: xTRα f, 5′-CTA CGA TCC AGA CAG CGA GAC-3′; xTRα r, 5′- GTT CAA AGG CGA GAA GGT AGG-3′; xTRβ f, 5′- ATG GCA ACA GAC TTG GTT TTG-3′; xTRβ r, 5′- CGC ATT AAC TAT GGG AGC TTG-3′; xBTEB f, 5′-CCA TCT CAA AGC CCA CTA CAG-3′; xBTEB r, 5′- GAA TTG GAC CTT TTG GAC CTT-3′.

Supporting information available: This material is free of charge *via* the Internet.

REFERENCES

1. Scanlan, T., Yoshihara, H., Nguyen, N.-H., and Chiellini, G. (2001) Selective thyromimetics: tissue-selective thyroid hormone analogs, *Curr. Opin. Drug Discovery Dev. 4*, 614–622.

2. Ocasio, C., and Scanlan, T. (2005) Clinical prospects for new thyroid hormone analogues, *Curr. Opin. Endocrinol. Diabetes 12*, 363–370.

3. Morkin, E., Ladenson, P., Goldman, S., and Adamson, C. (2004) Thyroid hormone analogs for treatment of hypercholesterolemia and heart failure: past, present, and future prospects, *J. Mol. Cell. Cardiol. 37*, 1137–1146.

4. Greenspan, F. S., and Gardner, D. G. (2001) The thyroid gland, in *Basic and Clinical Endocrinology* (Greenspan, F., Ed.) 6th ed., pp 201–272, Lange Medical Books/McGraw-Hill, New York.

5. Lazar, M. (1993) Thyroid hormone receptors: multiple forms, multiple possibilities, *Endocr. Rev. 14*, 184–193.

6. Brent, G. (2000) Tissue-specific actions of thyroid hormone: insights from animal models, *Rev. Endocr. Metab. Disord. 1*, 27–33.

7. Chiellini, G., Apriletti, J., Yoshihara, H., Baxter, J., Ribeiro, R., and Scanlan, T. (1998) A high-affinity subtype-selective agonist ligand for thyroid hormone receptor, *Chem. Biol. 5*, 299–306.

8. Borngraeber, S., Budny, M.-J., Chiellini, G., Cunha-Lima, S., Togashi, M., Webb, P., Baxter, J., Scanlan, T., and Fletterick, R. (2003) Ligand selectivity by seeking hydrophobicity in the thyroid hormone receptor, *Proc. Natl. Acad. Sci. U.S.A. 100*, 15358–15363.

9. Hayashi, M., Ohnota, H., Tamura, T., Kuroda, J., Shibata, N., Akahane, M., Moriwaki, H., Machida, N., and Mitsumori, K. (2004) Inhibitory effects of KAT-681, a liver-selective thyromimetic, on development of hepatocellular proliferative lesions in rats induced by 2-acetylaminofluorene and partial hepatectomy after diethylnitrosamine initiation, *Arch. Toxicol. 78*, 460–466.

10. Dow, R., Schneider, S., Paight, E., Hank, R., Chiang, P., Cornelius, P., Lee, E., Newsome, W., Swick, A., Spitzer, J., Hargrove, D., Patterson, T., Pandit, J., Chrunyk, B., LeMotte, P., Danley, D., Rosner, M., Ammirati, M., Simons, S., Schulte, G., Tate, B., and DaSilva-Jardine, P. (2003) Discovery of a novel series of 6-azauracil-based thyroid hormone receptor ligands: potent, TRβ subtype-selective thyromimetics, *Bioorg. Med. Chem. Lett. 13*, 379–382.

11. Ebisawa, M., Inoue, N., Fukasawa, H., Sotome, T., and Kagechika, H. (1999) Thiazolidinediones with thyroid hormone receptor agonistic activity, *Chem. Pharm. Bull. 47*, 1348–1350.

12. Hangeland, J., Friends, T., Doweyko, A., Mellström, K., Sandberg, J., Grynfarb, M., and Ryono, D. (2005) A new class of high affinity thyromimetics containing a phenyl-napthylene core, *Bioorg. Med. Chem. Lett. 15*, 4579–4584.

13. Chiang, Y.-C. (Pfizer Products Inc., USA) Preparation of [(hydroxyphenoxy)benzyl]thiazolidinediones and analogs as thyroid receptor ligands. *Eur. Pat. Appl.* EP-1148054, 17 Apr 2004.

14. Collazo, A.-M., Koehler, K., Garg, N., Färnegårdh, M., Husman, B., Ye, L., Ljunggren, J., Mellström, K., Sandberg, J., Grynfarb, M., Ahola, H., and Malm, J. (2006) Thyroid receptor ligands. Part 5: Novel bicyclic agonist ligands selective for the thyroid hormone receptor β, *Bioorg. Med. Chem. Lett. 16*, 1240–1244.

15. Hanig, H., Woltering, M., Mueller, U., Schmidt, G., Schmeck, C., Voehringer, V., Kretschmer, A., and Pernerstorfer, J. (2005) Novel heterocyclic thyromimetics, *Bioorg. Med. Chem. Lett. 15*, 1835–1840.

16. Kaltenbach, J. C. (1996) Endocrinology of amphibian metamorphosis, in *Metamorphosis postembryonic reprogramming of gene expression in amphibian and insect cells* (Gilbert, L., Tata, J., and Atkinson, B., Eds.), pp 403–431, Academic Press, San Diego, CA.

17. Furlow, J., Yung-Yang, H., Hsu, M., Lim, W., Ermio, D., Chiellini, G., and Scanlan, T. (2004) Induction of larval tissue resorption in *Xenopus laevis* tadpoles by the thyroid hormone receptor agonist GC-1, *J. Biol. Chem. 279*, 26555–26562.

18. Lim, W., Nguyen, N.-H., Yang, H., Scanlan, T., and Furlow, J. (2002) A thyroid hormone antagonist that inhibits thyroid hormone action *in vivo*, *J. Biol. Chem. 277*, 35664–35670.

19. Wang, Z., and Brown, D. (1993) Thyroid hormone-induced gene expression program for amphibian tail resorption, *J. Biol. Chem. 268*, 16270–16278.

20. Hart, M., Suchland, K., Miyakawa, M., Bunzow, J., Grandy, D., and Scanlan, T. (2006) Trace amine receptor-associated agonists: synthesis and evaluation of thyronamines and related analogues, *J. Med. Chem. 49*, 1101–1112.

21. Hodnett, N. (2003) Trimethylsilyldiazomethane, *Synlett 13*, 2095–2096.

22. Yoshihara, H., Apriletti, J., Baxter, J., and Scanlan, T. (2001) A designed antagonist of the thyroid hormone receptor, *Bioorg. Med. Chem. Lett. 11*, 2821–2825.

23. Evans, D., Katz, J., and West, T. (1998) Synthesis of diaryl ethers through the copper-promoted arylation of phenols with arylboronic acids - an expedient synthesis of thyroxine, *Tetrahedron Lett. 39*, 2937–2940.

24. Mishra, A., Panwar, P., Chopra, M., Sharma, R., and Chatal, J. (2003) Synthesis of novel bifuntional Schiff-base ligands derived from condensation of 1-(*p*-nitrobenzyl)ethylenediamine and 2-(*p*-nitrobenzyl)-3-monooxo-1,4,7-triazaheptane with salicylaldehyde, *New J. Chem. 27*, 1054–1058.

25. Yamaguchi, J., Harada, M., Kondo, T., Noda, T., and Suyama, T. (2003) A facile method for preparation of optically active hydantoin, *Chem. Lett. 32*, 372–373.

26. Apriletti, J., Baxter, J., Lau, K., and West, B. (1995) Expression of the Rat α1 Thyroid Hormone Receptor Ligand Binding Domain in *Escherichia coli* and the Use of a Ligand-Induced Conformation Change as a Method for Its Purification to Homogeneity, *Protein Expression Purif. 6*, 363–370.

27. Chiellini, G., Nguyen, N.-H., Yoshihara, H., and Scanlan, T. (2000) Improved synthesis of the iodine-free thyromimetic GC-1, *Bioorg. Med. Chem Lett. 10*, 2607–2611.

28. Nguyen, N.-H., Apriletti, J., Cunha-Lima, S., Webb, P., Baxter, J., and Scanlan, T. (2002) Rational design and synthesis of a novel thyroid hormone antagonist that blocks coactivator recruitment, *J. Med. Chem. 45*, 3310–3320.

29. Nieuwkoop, P. D., and Faber, J. (1994) *Normal Table of Xenopus Laevis (Daudin): A Systematical and Chronological Survey of the Development From the Fertilized Egg Till the End of Metamorphosis*, 2nd ed., Garland Publishing, New York and London.

30. Li, H. C. (1978) *Hormonal Proteins and Peptides*, 6th ed., Academic Press, New York.